

TECHNICAL  
REPORTS: METHODS

10.1002/2014GC005547

## Key Points:

- CRM is reliable tool to visualize internal growth patterns in modern and fossil shells
- CRM-based growth data suitable for cross-dating applications
- CRM recommended for samples with subsequent geochemical analysis

## Correspondence to:

L. Beierlein,  
lars.beierlein@awi.de

## Citation:

Beierlein, L., G. Nehrke, and T. Brey (2015), Confocal Raman microscopy in sclerochronology: A powerful tool to visualize environmental information in recent and fossil biogenic archives, *Geochem. Geophys. Geosyst.*, 16, doi:10.1002/2014GC005547.

Received 18 AUG 2014

Accepted 21 DEC 2014

Accepted article online 9 JAN 2015

## Confocal Raman microscopy in sclerochronology: A powerful tool to visualize environmental information in recent and fossil biogenic archives

Lars Beierlein<sup>1</sup>, Gernot Nehrke<sup>1</sup>, and Thomas Brey<sup>1</sup><sup>1</sup>Alfred Wegener Institute Helmholtz Centre for Polar and Marine Research, Bremerhaven, Germany

**Abstract** Biological hard parts and skeletons of aquatic organisms often archive information of past environmental conditions. Deciphering such information forms an essential contribution to our understanding of past climate conditions and thus our ability to mitigate the climatic, ecological, and social impacts of a rapidly changing environment. Several established techniques enable the visualization and reliable use of the information stored in anatomical features of such biogenic archives, i.e., its growth patterns. Here, we test whether confocal Raman microscopy (CRM) is a suitable method to reliably identify growth patterns in the commonly used archive *Arctica islandica* and the extinct species *Pygocardia rustica* (both Bivalvia). A modern *A. islandica* specimen from Norway has been investigated to verify the general feasibility of CRM, resulting in highly correlated standardized growth indices ( $r > 0.96$ ;  $p < 0.0001$ ) between CRM-derived measurements and measurements derived from the established methods of fluorescence microscopy and Mutvei's solution staining. This demonstrates the general suitability of CRM as a method for growth pattern evaluation and cross-dating applications. Moreover, CRM may be of particular interest for paleoenvironmental reconstructions, as it yielded superior results in the analysis of fossil shell specimens (*A. islandica* and *P. rustica*) compared to both Mutvei staining and fluorescence microscopy. CRM is a reliable and valuable tool to visualize internal growth patterns in both modern and fossil calcium carbonate shells that notably also facilitates the assessment of possible diagenetic alteration prior to geochemical analysis without geochemically compromising the sample. We strongly recommend the CRM approach for the visualization of growth patterns in fossil biogenic archives, where conventional methods fail to produce useful results.

## 1. Introduction

Detailed understanding of the global dynamics that have driven past environment and climate conditions prior to the era of instrumental and observational data (i.e., the last 200 years) is of utmost significance for proper forecasts of future climate development, e.g., by means of global coupled ocean-atmosphere models. Different archives of past climates contribute to this understanding of past climatic conditions and can subsequently be used to verify and improve models of future climate conditions. Commonly used archives such as sediment cores or ice cores cover long time spans (tens of thousands to millions of years, e.g., *Petit et al.* [1999]) but have limited temporal resolution (annual at best, but usually in the range of decades to thousands of years, e.g., *Hald et al.* [2007]). However, the reliability of paleoenvironmental/climate reconstructions and models can be greatly enhanced by including data on short-term variability at subdecadal or even subannual (e.g., seasonal) scales. Such information can be derived from nonbiogenic (e.g., speleothems) and biogenic (e.g., durable accretion parts of plants and animals) archives. The aquatic realm is a particularly rich resource of biogenic archives (mostly calcium carbonate) produced by long-lived organisms such as coralline algae, corals, mollusks, and fish (otoliths). These archives provide high-resolution information on decadal [*DeLong et al.*, 2007] and subannual [*Halfar et al.*, 2008] scales, while individual specimens can reach ages of several centuries [*Butler et al.*, 2013].

Bivalves constitute archives of increasing importance [*Richardson*, 2001; *Schöne*, 2013]. They can be found in almost all aquatic systems worldwide, but notably in boreal and polar regions where they represent the only available long-lived biogenic information source [*Schöne*, 2013]. Due to their annual resolution, analysis of the internal growth patterns in different bivalve species have been used successfully to identify multiyear and decadal oscillation patterns such as the North Atlantic Oscillation (NAO); [*Brocas et al.*, 2013], Arctic

Climate Regime Index (ACRI) [Carroll *et al.*, 2011], or El Niño Southern Oscillation (ENSO) [Schöne *et al.*, 2007]. Bivalve sclerochronology has additionally been used to identify multidecadal climate trends [Brey *et al.*, 2011], subannual environmental patterns (L. Beierlein *et al.*, The seasonal water temperature cycle in the Arctic Dicksonfjord (Svalbard) during the Holocene Climate Optimum derived from *Arctica islandica* shells, submitted to *The Holocene*, 2014) and has successfully been applied in archaeological studies, where, for example, bivalve shells from shell middens (mounds of discarded shell materials at prehistoric settlements) are used to identify seasonal patterns of resource procurement [Burchell *et al.*, 2013; Hallmann *et al.*, 2013].

The bivalve *Arctica islandica* is a unique biogenic archive of particular importance [Schöne, 2013] due to its longevity (400 years and more; [Butler *et al.*, 2013]), its wide boreal distribution throughout the North Atlantic [Dahlgren *et al.*, 2000] and the fact that it records environmental conditions of the ambient water on a subannual scale [Schöne and Fiebig, 2009].

To reliably utilize the climate and environmental information recorded within the shell, the internal growth pattern of the shell needs to be visualized. This is an absolute prerequisite for the successful compilation of master-chronologies and cross-dating applications (e.g., [Butler *et al.*, 2010]). Changes in carbonate structure and/or shell organic matter content are formed at regular intervals, and it is crucial to successfully couple and interpret the temporal and physical/biological mechanisms involved in these successive growth increments (for example annual, lunar, daily, tidal periodicity) in order to make reliable interpretations about past environments.

It is therefore essential that the accretionally precipitated growth increments within the shell are identified reliably and unambiguously, measured, and finally interpreted as a proxy for past environmental conditions. However, depending on the archive material (e.g., biogenic apatite or calcium carbonate), its age and preservation, it can be challenging to accurately and consistently reveal such information.

Several techniques have been established to visualize growth increments in sectioned bivalve shells. Common approaches are acetate peel replicas [Ropes, 1987] and treatment with Mutvei's solution [Schöne *et al.*, 2005a], which stains the organic compounds of the shell and simultaneously removes surface carbonate to create a relief structure. More technically sophisticated methods include fluorescence microscopy [Wanamaker *et al.*, 2009], which enhances contrast by inducing autofluorescence in organic compounds, backscattered electron microscopy (BSE) [Karney *et al.*, 2011], where the detection of backscattered high-energy electrons is used, and NanoSIMS [Karney *et al.*, 2012], which identifies differences in composition of annual growth increments.

Each of these methods has inherent advantages and limitations. Most preparation techniques are considered time consuming. Some are considered to make the unambiguous identification of growth increments difficult (acetate peels), require etching of the shell surface (i.e., the cross section will become unusable for geochemical analysis) or require different steps of shell pretreatment (e.g., spattering). Mutvei's solution uses glutaraldehyde (for chemical fixation of organic compounds), which is a hazardous respiratory toxin. In addition, most of the commonly used techniques are only of limited use when applied to fossil shell material. This also applies for Mutvei's solution, where smaller amounts of polysaccharides are present in the skeletons of older shells result in reduced contrast and lighter staining [Schöne *et al.*, 2005a].

Raman spectroscopy is a commonly applied technique in geosciences (e.g., for the identification and characterization of minerals) and studies of biominerals [Nehrke and Nouet, 2011; Wall and Nehrke, 2012]. Confocal Raman microscopy (CRM) has been employed in several biological studies involving mollusks, for example it has been used in studies to identify polyenes/pigments in several bivalve species [Barnard and de Waal, 2006; Hedegaard *et al.*, 2006; Stemmer and Nehrke, 2014], to demonstrate that changes in the biomineralization of the Peruvian bivalve *Trachycardium procerum* are associated with El Niño events [Perez-Huerta *et al.*, 2013], to document meteoric diagenesis involving syntaxial overgrowth of aragonite cement on late Pleistocene aragonitic freshwater bivalve biocrystals [Webb *et al.*, 2007], and for polymorph identification in marine and freshwater bivalve shells and pearls [Wehrmeister *et al.*, 2010; Nehrke *et al.*, 2012].

Here we test whether CRM is a suitable or even superior—in terms of resolution and efficiency—tool for visualizing internal shell growth patterns compared to Mutvei's solution and fluorescence microscopy, using shells of *A. islandica* and *Pygocardia rustica* and with particular emphasis on fossil specimens. We

**Table 1.** Modern and Fossil Shell Specimens Analyzed in This Study

Shell ID	Species	Ontogenetic		Location	Epoch/Stage/Age	Collected in	Shell Provider
		Age (Years)					
Ai1276R	<i>A. islandica</i>	65		Tromsø, Norway	Modern	2006	S. Begum (AWI Bremerhaven)
Al-CoCr-01	<i>A. islandica</i>	31		Sudbourne Park Pit, UK	Pliocene/Coralline Crag/Ramsholt Member	1974/1975	P. E. Long (Univ. of Leicester)
Al-StRi-BK1b	<i>A. islandica</i>	not determined		Stirone River, Italy	Pleistocene/ Middle Calabrian	2011	D. Scarponi, S. Raffi (Univ. of Bologna)
RGM609.096	<i>P. rustica</i>	17		Antwerp, Belgium	Pliocene/Piacenzian/ Lillo Formation, Oorderen Member	1958	F. Wesselingh (Naturalis, Leiden)

additionally discuss and evaluate the advantages and limitations of CRM in comparison to other visualization techniques.

## 2. Materials and Methods

### 2.1. Origin and Preparation of Shell Material

A total of four shell specimens have been analyzed in this study (for detailed information on shell material see Table 1). We test the CRM approach against the established methods of Mutvei staining and fluorescence microscopy (FL) using one modern *Arctica islandica* shell (ID: Ai1276R) from Tromsø, Norway. Then we compared the performance of the three methods with fossil shells, using two fossil *A. islandica* shells (IDs: Al-CoCr-01 from Sudbourne Park Pit, UK; Al-StRi2-BK1b from Stirone River, Italy) and one fossil *Pygocardina rustica* shell (ID: RGM609.096 from Antwerp, Belgium).

*A. islandica* builds its three shell layers out of aragonite [Schöne, 2013] as does the extinct species *P. rustica*, which inhabited a similar ecological niche as *A. islandica* [Bosch and Wesselingh, 2006]. Annual growth lines in both taxa are usually precipitated in autumn and winter [Ropes et al., 1984].

All four shells were initially covered with an epoxy resin and cut using a low-speed precision saw (Buehler, IsoMet) equipped with a 0.4 mm diamond-coated saw blade. Cross sections of 3 mm thickness were cut perpendicular to the growth lines, glued on glass slides and ground using a manual grinder (Buehler, Phoenix Alpha), and sand paper with three different grain sizes (15, 10, and 5  $\mu\text{m}$ ). All shells have been analyzed consecutively, starting with the FL method then the CRM method and finally the Mutvei staining approach.

### 2.2. Visualization Methods

#### 2.2.1. Confocal Raman Microscopy (CRM)

In contrast to elastic light scattering (also known as Rayleigh scattering), which applies to the main fraction of light, a very small fraction of incident light is scattered inelastically (commonly termed Raman scattering) [Raman and Krishnan, 1928]. The resulting difference in frequency between irradiated and scattered light (Stokes shift) depends on the specific molecular vibration of the molecules and can therefore be used for material identification [e.g., Smith and Dent, 2005]. All shells analyzed in this study consist of aragonite, which is identified based on two lattice modes (translation mode, 152  $\text{cm}^{-1}$  and liberation mode, 206  $\text{cm}^{-1}$ ) and the two vibration modes (C–O symmetric stretch, 1085  $\text{cm}^{-1}$  and C–O in-plane bending, 705  $\text{cm}^{-1}$ ).

We used a confocal Raman microscope (CRM) (WITec alpha 300 R) with two different monochromatic light sources (diode lasers): a laser with an excitation wavelength of 488 nm (pinhole size: 50  $\mu\text{m}$ ) and one of 785 nm (pinhole size: 100  $\mu\text{m}$ ) in conjunction with a motorized scan table with a maximum scan range of 2.5  $\times$  2.5 cm and a minimum step size of 100 nm. Raman maps were taken using 20 $\times$  (Zeiss EC Epiplan, NA = 0.4) and 100 $\times$  (Nikon, NA = 0.9) objectives. Raman signals were detected using a UHTS300 ultra high throughput spectrometer (WITec GmbH, Ulm, Germany) in which the spectrometer for 488 nm excitation wavelengths used a 600  $\text{mm}^{-1}$  grating and a 500 nm blaze while the spectrometer for 785nm excitation wavelength used a 600  $\text{mm}^{-1}$  grating and a 750 nm blaze. Subsequent spectral analysis and processing of digital images were conducted using WITecProject software (version 2.10, WITec GmbH, Ulm, Germany). Integration time was chosen to 0.1 s, while all measurements have been conducted at room temperature.

In order to establish whether the obtained results from Raman mapping are comparable to more commonly used techniques such as fluorescence microscopy (from here on referred as FL) [Wanamaker et al., 2009]

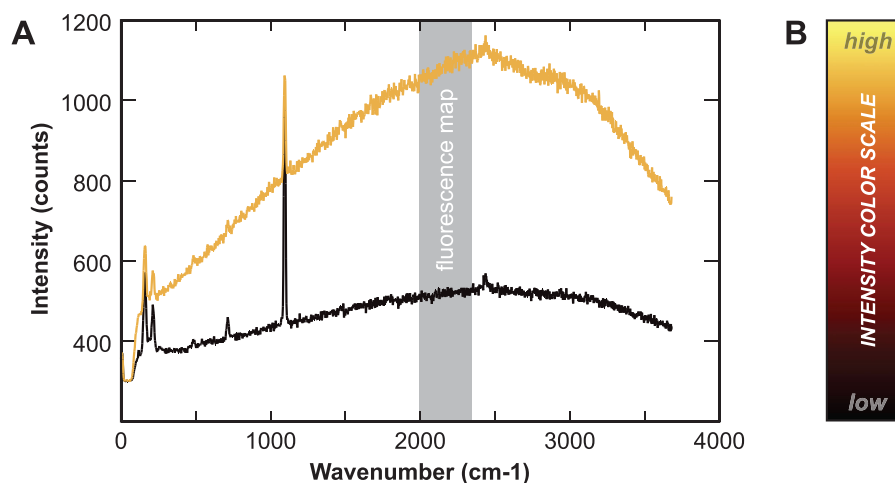


**Figure 1.** Color-coding in CRM fluorescence maps. (a) Two exemplary Raman-derived spectra for aragonite. The relative intensity difference in the spectral region 2000–2400  $\text{cm}^{-1}$  is used to derive fluorescence maps. (b) High relative intensities (yellow) and low relative intensities (black) define the “color coding” range of the fluorescence maps (as seen in Figures 2, 3, 4, and 6).

and staining with Mutvei’s solution [Schöne *et al.*, 2005a], a mapping approach was applied [cf., Nehrke and Nouet, 2011; Nehrke *et al.*, 2012; Wall and Nehrke, 2012; Stemmer and Nehrke, 2014], where each pixel consists of a single spectrum containing the entire spectral information (Figure 1). Raman maps in this study are large area scans showing the relative intensity difference of the fluorescence signal between wave numbers of 2000 and 2400  $\text{cm}^{-1}$  before any background subtraction was applied (Figure 1a). Consequently, and following descriptions in Nehrke and Nouet [2011] and Wall and Nehrke [2012], we use the fluorescence intensity distribution to map the distribution of organic components. Intensity color-coding has been chosen as orange and red (compare Figure 1b).

### 2.2.2. Fluorescence Microscopy

Following the recommendations in Wanamaker *et al.* [2009], we used the “blue light spectrum” where internal growth lines of the hinge plate become most prominent. An excitation filter (BP 460–490; excitation 460–490 nm, emission 515 nm) and a barrier filter (BA510IF), filtering the reflected light, were used. Images were taken in analysis docu software (Olympus, version 5.1) using a stereomicroscope (Olympus, SZX12) attached to a CCD camera (Olympus, U-CMAD).

### 2.2.3. Mutvei’s Solution

The application of Mutvei’s solution to shells or skeletons simultaneously causes chemical etching (acetic acid), histochemical staining (alcian blue) and chemical fixation (glutaraldehyde). Cross sections of three shell specimens (IDs: Ai1276R, Al-CoCr-01, and RGM609.096) were stained with Mutvei’s solution according to the procedure described in Schöne *et al.* [2005a]. An immersion time of 23 minutes at 37–40°C has been applied. Due to unsatisfactory results in the fossil specimens, immersion times were stepwise increased to 46 min in specimen RGM609.096 and 60 min in specimen Al-CoCr-01. Digital images of Mutvei stained cross sections were taken using an Olympus SZX12 stereomicroscope equipped with an Olympus U-CMAD CCD camera and analysis docu software (Olympus, version 5.1).

### 2.3. Growth Increment Measurements

We determined increment widths in the aragonitic hinge plates of three shells, a modern *A. islandica* (ID: Ai1276R; Figure 2), a fossil *A. islandica* (ID: Al-CoCr-01; Figure 3), and a fossil *P. rustica* (ID: RGM609.096; Figure 4). Increment width in CRM maps as well as in Mutvei and FL derived images was measured using Panopea image processing software (© Peinl & Schöne). Mutvei-derived and FL-derived images were processed with Adobe Photoshop (version CS5.1) in order to enhance contrast and guarantee comparable results. Increment series were transformed into standardized growth index (SGI) series by means of detrending using a cubic spline ( $\lambda = 150$ ; JMP statistical software, version 9.0.1, SAS Institute Inc. 2007) and subsequent calculation of SGI following Schöne *et al.* [2005b]. We compared the SGI series obtained by CRM, FL and Mutvei staining, following the approach of Wanamaker *et al.* [2009].

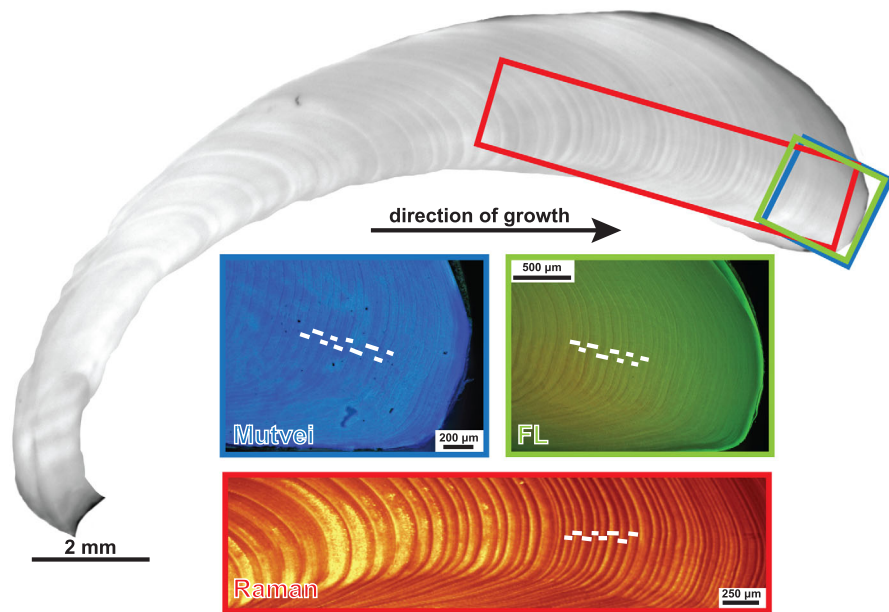


**Figure 2.** Verification approach: Growth increments in the hinge plate of the modern *A. islandica* shell specimen (ID: Ai1276R) were successfully visualized, counted, and measured using Mutvei staining (blue), FL (green), and CRM mapping (red). White lines indicate increment widths, perpendicular to the annual growth lines. CRM measurements taken with an excitation wavelength of 488 nm.

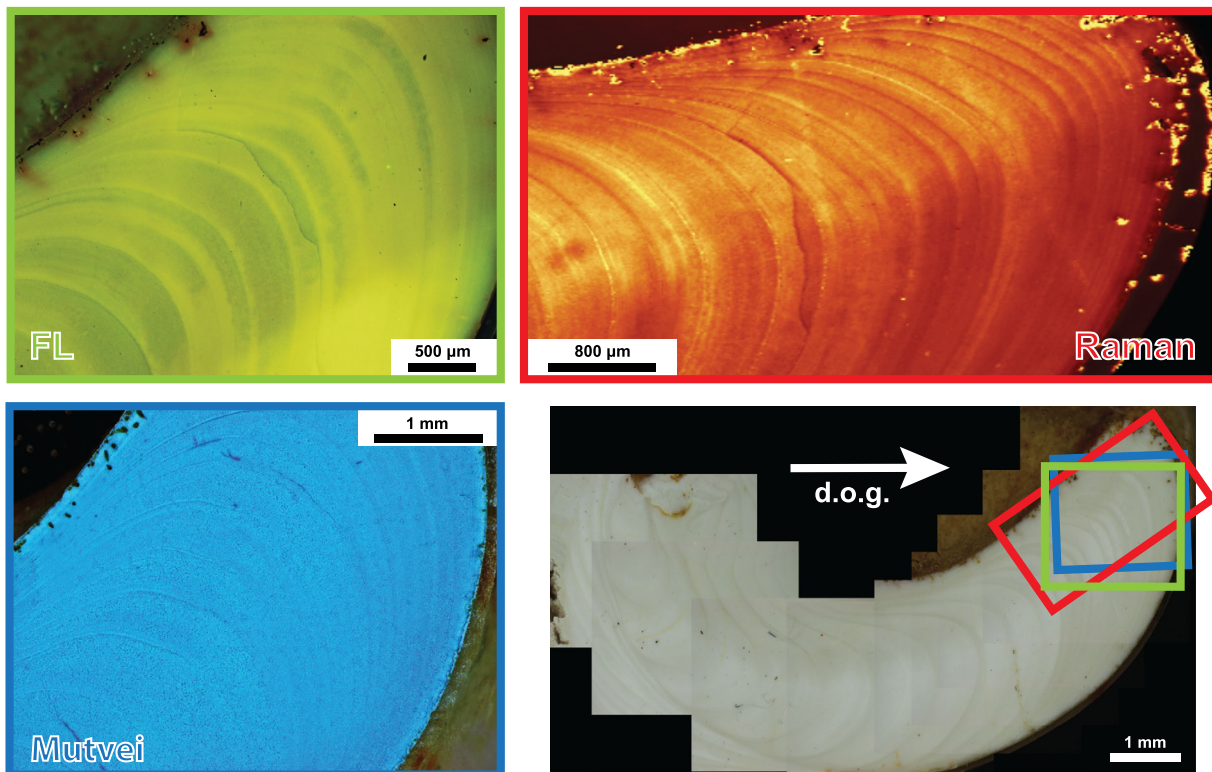


**Figure 3.** Hinge plate of fossil *A. islandica* specimen AI-CoCr-01 analyzed by FL (green), Mutvei staining (blue), and CRM mapping (red). FL and Mutvei staining approaches do not allow for distinction of growth increments in the ontogenetically oldest parts of the shell carbonate, but CRM maps do. CRM measurements taken with an excitation wavelength of 785 nm. Arrow indicates direction of growth (d.o.g.).

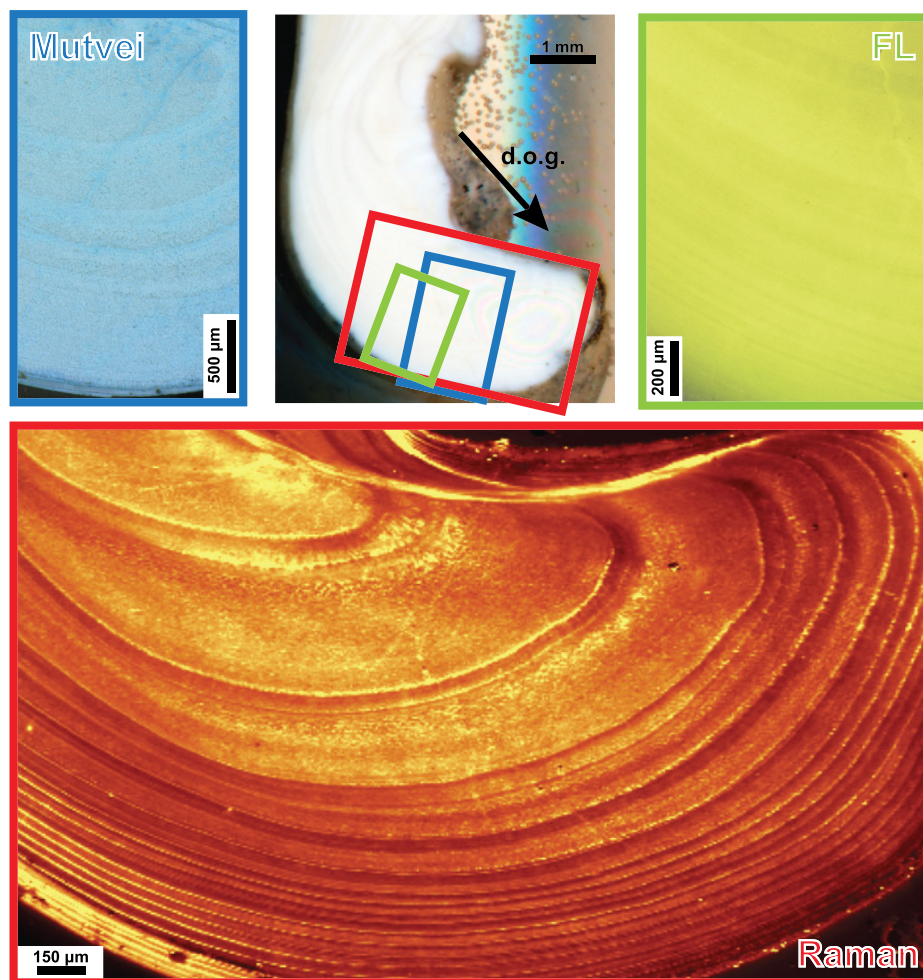


**Figure 4.** Hinge plate of fossil *P. rustica* specimen RGM609.096 analyzed by Mutvei staining (blue), FL (green), and CRM mapping (red). FL and Mutvei staining approaches do not allow for distinction of growth increments in the ontogenetically oldest parts of the shell carbonate, but CRM maps do. CRM measurements taken with an excitation wavelength of 785 nm. Arrow indicates direction of growth (d.o.g.).

### 3. Results

#### 3.1. CRM Verification With Modern *A. islandica* Shell

We were able to identify, count, and measure internal growth increments throughout the entire hinge plate of the modern *A. islandica* shell specimen Ai1276R (Figure 2) on digital photographs derived from the Mutvei and FL approaches as well as on CRM maps. The corresponding growth increment time series (Figure 5a) were detrended and standardized growth indices (SGI) were calculated (Figure 5b). The CRM SGI series correlates strongly with the FL series ( $r = 0.98$ ;  $p < 0.0001$ ;  $N = 57$ ; age 5–62) and the Mutvei series ( $r = 0.96$ ;  $p < 0.0001$ ;  $N = 57$ ; age 5–62) and the same applies to the Mutvei and FL series ( $r = 0.97$ ;  $p < 0.0001$ ;  $N = 57$ ; age 5–62). Specimen Ai1276R became 65 ontogenetic years old, covering a life span from 1942 to 2006 (Figures 5a and 5b). For the verification approach, the time span from 1946 to 2003 was chosen.

#### 3.2. Application to Fossil *A. islandica* and *P. rustica*

CRM maps clearly show annual growth increments throughout the entire hinge plate (Figures 3 and 4). Based on these maps, the Pliocene *A. islandica* specimen (AI-CoCr-01) reached an ontogenetic age of 31 years (Figure 5c) while the Pliocene *P. rustica* specimen (ID: RGM609.096) reached an age of 17 years (Figure 5e). The FL and Mutvei staining approaches of both fossil specimens resulted in digital images of very low contrast (Figures 3 and 4). Particularly in the ontogenetically older areas, where growth increments become most narrow, a clear distinction between increments was no longer possible. Consequently, it was not possible to reliably measure the internal growth pattern over the entire hinge plate (Figures 5c–5f). The Mutvei

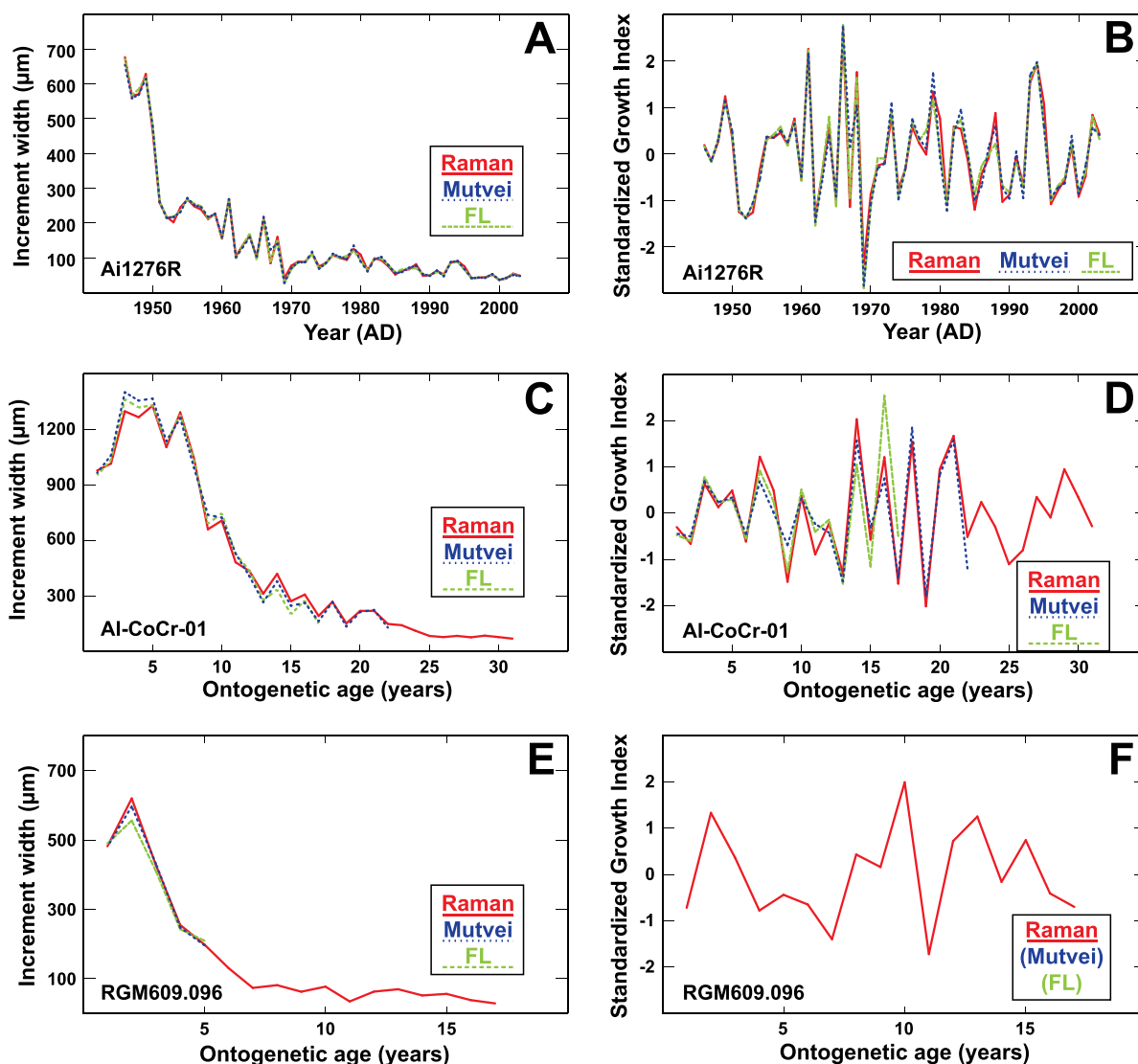


**Figure 5.** Comparison of growth increment series in modern *A. islandica* (ID: Ai1276R) (a), fossil *A. islandica* (ID: Al-CoCr-01) (c) and fossil *P. rustica* (ID: RGM609.096) (e) as determined by means of FL (green-dashed line), Mutvei staining (blue-dotted line) and CRM (red solid line). SGI series for Ai1276R (N = 57; age 5–62; b) correlate significantly between CRM and FL ( $r = 0.98$ ;  $p < 0.0001$ ), between CRM and Mutvei ( $r = 0.96$ ;  $p < 0.0001$ ) and between Mutvei and FL ( $r = 0.97$ ;  $p < 0.0001$ ). SGI series for Al-CoCr-01 (d) correlate significantly between CRM (31 years) and FL (17 years) for the first 17 years ( $r = 0.86$ ;  $p < 0.0001$ ) and between Mutvei (22 years) and CRM for the first 22 years ( $r = 0.95$ ;  $p < 0.0001$ ). Due to short FL (5 years) and Mutvei staining (5 years) derived time-series in RGM609.096, SGI (f) has only been calculated for CRM approach (solid red line). Colors and lines as a, c, e.

treatment revealed the first 22 ontogenetic years only, and the FL treatment the first 17 years in the fossil *A. islandica* specimen (Figures 5c and 5d). In the fossil *P. rustica* specimen (ID: RGM609.096), both Mutvei and FL treatment showed the first five ontogenetic years only (Figures 5e and 5f). In the Pliocene *A. islandica* specimen (Al-CoCr-01), SGI series obtained by CRM and Mutvei (22 years;  $r = 0.95$ ;  $p < 0.0001$ ) as well as by CRM and FL (17 years;  $r = 0.86$ ;  $p < 0.0001$ ) are strongly correlated (Figure 5d). The short increment series obtained with FL and Mutvei treatments did not allow for a corresponding SGI series comparison for Pliocene *P. rustica* specimen (Figure 5f).

## 4. Discussion

### 4.1. Verification on Modern *A. islandica*

The strong correlations ( $r > 0.96$ ;  $p < 0.0001$ ) between SGI series resulting from CRM, FL, and Mutvei treatments (Figure 5b) confirm that the shell growth increment pattern visualized by CRM mapping is identical to the growth patterns detected by the established methods Mutvei staining and FL. Therefore, CRM can be considered to be an equally reliable method to visualize internal growth structures in aragonite shells. It is also

suitable for cross-dating applications such as the compilation of master chronologies, where the growth records of single specimens with overlapping life spans are stacked to produce a compilation of environmental change that can cover time spans of up to several hundred years [Butler *et al.*, 2013]. Consequently, such archives allow for climatic reconstructions from a daily to a multidecadal or even centennial time scale.

#### 4.2. Analysis of Fossil *A. islandica* and *P. rustica*

In both the fossil *A. islandica* (ID: Al-CoCr-01) and the fossil *P. rustica* (ID: RGM609.096) shell, the two commonly used techniques Mutvei staining and FL failed to visualize the complete shell growth pattern (Figures 5c–5f). The very low contrast of the preparations rendered it impossible to identify and measure increments in the ontogenetically oldest parts of the shells (Figures 3–5). Regarding the Mutvei treatment, even the extension of the exposition duration from 23 min to up to 60 min did not result in improved contrast. This finding confirms Schöne *et al.* [2005a], who state that Mutvei's solution results in lighter shadings of blue in fossil material. Schöne *et al.* [2005a] hypothesize that the low contrast in fossil specimens might be associated with diagenetic alteration of the shell material. However, CRM analysis indicates that the measured shell material consist solely of aragonite. Hence, a strong diagenetic alteration, resulting in the transformation of aragonite into the more stable polymorph calcite [e.g., Maliva and Dickson, 1992], can be excluded. However, taphonomic alteration processes might have led to reduced amounts of polysaccharides in the fossil shell material [cf., Schöne *et al.*, 2005a] being a more likely explanation of the weaker effect of the Mutvei treatment on fossil shells.

So far, we do not fully understand the cause-and-effect mechanisms that underlie the extraordinary good performance of CRM in fossil carbonate shell material. All three methods tested here rely in some way on the organic content of the shell. Since detailed studies of the organic composition of mollusk shells such as *A. islandica* and *P. rustica* are lacking, we cannot say which specific chemical compounds cause the fluorescence in FL and CRM. Scenarios with increasing organic composition [cf., Wanamaker *et al.*, 2009; Karney *et al.*, 2011] or mineralization (as described in Karney *et al.* [2011] for an elevated backscattered signal) prior to or during the formation of growth lines seem plausible. Both Mutvei staining and FL performed poorly when applied to fossil shell material, most likely owing to the decay and loss of shell organic compounds over time. In contrast to Mutvei staining and FL, CRM mapping seems to be able to visualize organic-related shell structures even after the original organic components have already been strongly altered.

#### 4.3. Potential of CRM in Sclerochronology

##### 4.3.1. Advantages and Limitations of CRM

We show that confocal Raman microscopy (CRM) can visualize internal growth patterns in both modern and fossil biogenic carbonate structures, showing a performance as good or even better than the established methods Mutvei staining and FL. Compared to established methods, CRM mapping offers a unique combination of features that make it the most versatile approach:

1. CRM analysis does not require chemical sample (pre-) treatment, i.e., the shell surface is neither contaminated nor destroyed. This is in contrast to Mutvei staining, acetate peels (surface etching), and BSE (sputtering with carbon, gold, or platinum), which modify the shell to enhance visibility of the micro structures. Furthermore, no toxic/hazardous chemicals are involved such as glutaraldehyde (a respiratory toxin) and alcian blue in Mutvei's solution. Consequently, shell cross-sections analyzed by CRM can be used for subsequent geochemical analysis (e.g., stable isotopes or trace/minor elements as shown in [Nehrke *et al.*, 2012]).
2. The CRM mapping area is large. Larger areas can be scanned consecutively (by moving the sample) and maps can be stitched (to a mosaic) afterwards.
3. CRM analysis can be conducted with high spatial resolution (down to several hundred nanometer), allowing the detection and identification of even finest growth structures (Figure 6). This is especially advantageous in the study of subannual variability.

Nevertheless, CRM has some limitations, too:

1. The confocal Raman microscope represents a relatively expensive instrument that may not yet be available easily.

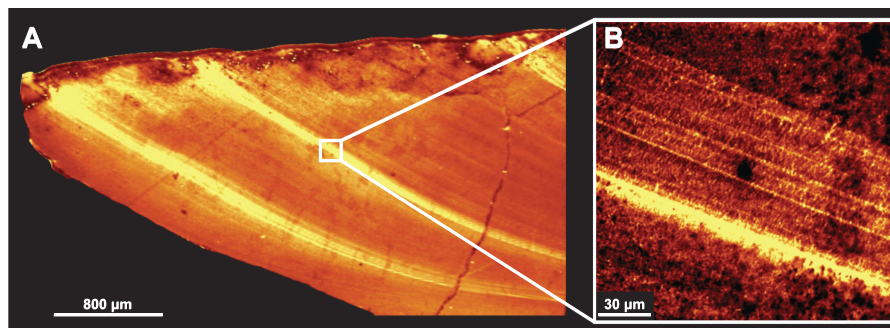


**Figure 6.** CRM maps of ventral shell margin in fossil *A. islandica* specimen AI-StRi2-BK1b. (a) CRM map using a 20 $\times$  magnification and showing two pronounced annual winter growth lines (yellow) at the (broken) ventral margin of the shell. (b) High-resolution CRM map of the area indicated in (A) using a 100 $\times$  magnification and showing intra-annual growth patterns within a single winter line.

2. Depending on scan area, resolution and integration time, a single scan can take several hours. Hence, at the current technical level, CRM mapping may not become the standard tool for growth increment analysis, but may serve best in cases where standard methods fail.
3. Caution is advised when exposing organic-rich samples to a laser source. Repeated measurements may dampen the Raman signal significantly. Furthermore, shell coatings such as polyvinyl alcohol (PVA) might burn when exposed to a monochromatic light source.

#### 4.3.2. Check for Diagenesis and Contamination

A check for taphonomic alteration (e.g., recrystallization from pristine aragonite to secondary calcite) in marine biogenic carbonates should be a mandatory step prior to any kind of biogeochemical analysis such as stable isotopes or trace elemental ratios of fossil samples. Therefore, CRM mapping can play a crucial role in the quality control of biogenic carbonate studies. *Nehrke et al.* [2012] highlighted the potential of CRM mapping in the identification of three different calcium carbonate polymorphs in the hinge plate of a modern marine bivalve species from Antarctica. In combination with electron microprobe (EMP) analysis, they were able to show that trace element incorporation differs with calcium carbonate polymorph (e.g., for magnesium and strontium). CRM may be helpful, too, in detecting contamination of shell material that might result from laboratory preparation (e.g., from glue or polishing residuals). Again, this check should be a mandatory step prior to any geochemical analysis.

## 5. Conclusions

In this study, we show that CRM is a reliable and valuable tool to visualize internal growth patterns in modern (Figures 2, 5a, and 5b) and fossil bivalve shell specimens of *A. islandica* (Figures 3, 5c, 5d, and 6) and *P. rustica* (Figures 4, 5e, and 5f). CRM performs as good as established methods (Mutvei staining and FL) in modern shells. Therefore, CRM based growth data are considered suitable for cross-dating applications, such as those used to compile master chronologies from multiple specimen archives. Regarding fossil shells, CRM reveals growth patterns where established methods fail, thus enabling a much more precise record of annual and even subannual growth increments (Figure 6) and the interpretation of their palaeoenvironmental information (Figures 5d and 5f). Furthermore, CRM constitutes an alternative nondestructive approach (as described for FL in *Wanamaker et al.* [2009]) that does not require any pretreatment of the shell cross section and makes the preparation of a second cross section for geochemical analysis redundant.

We strongly recommend the use of CRM in samples where further geochemical analysis will be undertaken and as the best technique available for the imaging of annual growth increments in fossil bivalve shells. We emphasize that CRM should be considered a powerful tool for assessing the absence or degree of diagenetic alteration in fossil carbonate shell specimens prior to any geochemical analysis.

## 6. Outlook

Future studies based on CRM mapping in sclerochronology should test for the potential to utilize high-resolution scans as shown in Figure 6 to visualize (daily or tidal) microincrements [*Schöne et al.* 2005c]. The

role and function of polyenes and pigments in the biomineralization processes of modern and fossil mollusk specimens needs to be better understood and their potential in terms of visualization of internal growth patterns needs to be tested. The method described here should also be applied to *A. islandica* specimens of older ontogenetic ages (100+ years), in the ventral portion of the shell and combined with studies on the organic content of *A. islandica* to decipher the origin of fluorescence variability. Application of this technique on additional mollusk taxa, both modern and fossil, and on noncarbonate palaeoarchives such as modern and fossil biogenic apatites (bones and teeth) or speleothems should be undertaken to fully test and exploit the potential of this versatile tool in archaeology and geosciences, as well as in climate-related proxy reconstructions.

### Acknowledgments

Data used to produce the results and figures in this study will be made available online (after publication) in PANGAEA® (<http://www.pangaea.de/>). The first author (L.B.) was financed by the "Earth System Science Research School (ESSReS)", an initiative of the Helmholtz Association of German Research Centres (HGF) at the Alfred Wegener Institute (AWI), Helmholtz Centre for Polar and Marine Research. We would like to thank Peter E. Long (University of Leicester), Daniele Scarponi, Sergio Raffi (both University of Bologna), and Frank Wesselingh (Naturalis Museum, Leiden) for providing the shell material. Further thanks to Rosie Sheward (NOC, Southampton) for suggestions that improved the written quality of the manuscript.

### References

- Barnard, W., and D. de Waal (2006), Raman investigation of pigmentary molecules in the molluscan biogenic matrix, *J. Raman Spectrosc.*, *37*, 342–352.
- Bosch, J., and F. Wesselingh (2006), On the stratigraphic position of the Delden Member (Breda Formation, Overijssel, the Netherlands) with implications for the taxonomy of *Pygocardia* (Mollusca, Bivalvia), *Cainozoic Res.*, *4*, 109–117.
- Brey, T., M. Voigt, K. Jenkins, and I.-Y. Ahn (2011), The bivalve *Laternula elliptica* at King George Island: A biological recorder of climate forcing in the West Antarctic Peninsula region, *J. Mar. Syst.*, *88*, 542–552.
- Brocas, W. M., D. J. Reynolds, P. G. Butler, C. A. Richardson, J. D. Scourse, I. D. Ridgway, and K. Ramsay (2013), The dog cockle, *Glycymeris glycymeris* (L.), a new annually-resolved sclerochronological archive for the Irish Sea, *Palaeogeogr. Palaeoclimatol. Palaeoecol.*, *373*, 133–140.
- Burchell, M., A. Cannon, N. Hallmann, H. P. Schwarcz, and B. R. Schöne (2013), Inter-site variability in the season of shellfish collection on the central coast of British Columbia, *J. Archaeol. Sci.*, *40*, 626–636.
- Butler, P. G., C. A. Richardson, J. D. Scourse, A. D. Wanamaker Jr, T. M. Shammon, and J. D. Bennell (2010), Marine climate in the Irish Sea: Analysis of a 489-year marine master chronology derived from growth increments in the shell of the clam *Arctica islandica*, *Quat. Sci. Rev.*, *29*, 1614–1632.
- Butler, P. G., A. D. Wanamaker Jr, J. D. Scourse, C. A. Richardson, and D. J. Reynolds (2013), Variability of marine climate on the North Icelandic Shelf in a 1357-year proxy archive based on growth increments in the bivalve *Arctica islandica*, *Palaeogeogr. Palaeoclimatol. Palaeoecol.*, *373*, 141–151.
- Carroll, M. L., W. G. Ambrose Jr, B. S. Levin, S. K. Ryan, A. R. Ratner, G. A. Henkes, and M. J. Greenacre (2011), Climatic regulation of *Clinocardium ciliatum* (bivalvia) growth in the northwestern Barents Sea, *Palaeogeogr. Palaeoclimatol. Palaeoecol.*, *302*, 10–20.
- Dahlgren, T. G., J. R. Weinberg, and K. M. Halanach (2000), Phylogeography of the ocean quahog (*Arctica islandica*): Influences of paleoclimate on genetic diversity and species range, *Mar. Biol.*, *137*, 487–495.
- DeLong, K. L., T. M. Quinn, and F. W. Taylor (2007), Reconstructing twentieth-century sea surface temperature variability in the southwest Pacific: A replication study using multiple coral Sr/Ca records from New Caledonia, *Paleoceanography*, *22*, PA4212, doi:10.1029/2007PA001444.
- Hald, M., C. Andersson, H. Ebbesen, E. Jansen, D. Klitgaard-Kristensen, B. Risebrobakken, G. R. Salomonsen, M. Sarnthein, H. P. Sejrup, and R. J. Telford (2007), Variations in temperature and extent of Atlantic Water in the northern North Atlantic during the Holocene, *Quat. Sci. Rev.*, *26*, 3423–3440.
- Halfar, J., R. S. Steneck, M. Joachimski, A. Kronz, and A. D. Wanamaker (2008), Coralline red algae as high-resolution climate recorders, *Geology*, *36*, 463–466.
- Hallmann, N., M. Burchell, N. Brewster, A. Martindale, and B. R. Schöne (2013), Holocene climate and seasonality of shell collection at the Dundas Islands Group, northern British Columbia, Canada: A bivalve sclerochronological approach, *Palaeogeogr. Palaeoclimatol. Palaeoecol.*, *373*, 163–172.
- Hedegaard, C., J.-F. Bardeau, and D. Chateigner (2006), Molluscan shell pigments: An in situ resonance Raman study, *J. Molluscan Stud.*, *72*, 157–162.
- Karney, G. B., P. G. Butler, J. D. Scourse, C. A. Richardson, K. H. Lau, J. T. Czernuszka, and C. R. M. Grovenor (2011), Identification of growth increments in the shell of the bivalve mollusc *Arctica islandica* using backscattered electron imaging, *J. Microsc.*, *241*, 29–36.
- Karney, G. B., P. G. Butler, S. Speller, J. D. Scourse, C. A. Richardson, M. Schröder, G. M. Hughes, J. T. Czernuszka, and C. R. M. Grovenor (2012), Characterizing the microstructure of *Arctica islandica* shells using NanoSIMS and EBSD, *Geochem. Geophys. Geosyst.*, *13*, Q04002, doi:10.1029/2011GC003961.
- Maliva, R. G., and J. A. D. Dickson (1992), The mechanism of skeletal aragonite neomorphism: Evidence from neomorphosed mollusks from the upper Purbeck Formation (Late Jurassic–Early Cretaceous), southern England, *Sediment. Geol.*, *76*, 221–232.
- Nehrke, G., and J. Nouet (2011), Confocal Raman microscope mapping as a tool to describe different mineral and organic phases at high spatial resolution within marine biogenic carbonates: Case study on *Nerita undata* (Gastropoda, Neritopsina), *Biogeosciences*, *8*, 3761–3769.
- Nehrke, G., H. Poigner, D. Wilhelms-Dick, T. Brey, and D. Abele (2012), Coexistence of three calcium carbonate polymorphs in the shell of the Antarctic clam *Laternula elliptica*, *Geochem. Geophys. Geosyst.*, *13*, Q05014, doi:10.1029/2011GC003996.
- Perez-Huerta, A., M. F. Etayo-Cadavid, C. F. T. Andrus, T. E. Jeffries, C. Watkins, S. C. Street, and D. H. Sandweiss (2013), El Niño Impact on Mollusk Biomineralization: Implications for trace element proxy reconstructions and the paleo-archaeological record, *PLOS One*, *8*, e54274.
- Petit, J. R., et al. (1999), Climate and atmospheric history of the past 420,000 years from the Vostok ice core, Antarctica, *Nature*, *399*, 429–436.
- Raman, C. V., and K. S. Krishnan (1928), A new type of secondary radiation, *Nature*, *121*, 501–502.
- Richardson, C. A. (2001), Molluscs as archives of environmental change, *Oceanogr. Mar. Biol.*, *39*, 103–164.
- Ropes, J. W. (1987), Preparation of acetate peels of valves from the ocean quahog, *Arctica islandica*, for age determinations, U.S. Dept. of Comm., NOAA, Washington, D. C.
- Ropes, J. W., D. S. Jones, S. A. Murawski, F. M. Serchuk, and A. Jearld Jr (1984), Documentation Of annual growth lines in ocean quahogs, *Arctica islandica* Linné, *Fish. Bull.*, *82*, 1–19.

- Schöne, B. R. (2013), *Arctica islandica* (Bivalvia): A unique paleoenvironmental archive of the northern North Atlantic Ocean, *Global Planet. Change*, *111*, 199–225.
- Schöne, B. R., and J. Fiebig (2009), Seasonality in the North Sea during the Allerød and Late Medieval Climate Optimum using bivalve sclerochronology, *Int. J. Earth Sci.*, *98*, 83–98.
- Schöne, B. R., E. Dunca, J. Fiebig, and M. Pfeiffer (2005a), Mutvei's solution: An ideal agent for resolving microgrowth structures of biogenic carbonates, *Palaeogeogr. Palaeoclimatol. Palaeoecol.*, *228*, 149–166.
- Schöne, B. R., J. Fiebig, M. Pfeiffer, R. Gle, J. Hickson, A. L. A. Johnson, W. Dreyer, and W. Oschmann (2005b), Climate records from a bivalved Methuselah (*Arctica islandica*, Mollusca; Iceland), *Palaeogeogr. Palaeoclimatol. Palaeoecol.*, *228*, 130–148.
- Schöne, B. R., S. D. Houk, A. D. Freyre Castro, J. Fiebig, W. Oschmann, I. Kröncke, W. Dreyer, and F. Gosselck (2005c), Daily growth rates in shells of *Arctica islandica*: Assessing sub-seasonal environmental controls on a long-lived bivalve mollusk, *Palaios*, *20*, 78–92.
- Schöne, B. R., N. Page, D. Rodland, J. Fiebig, S. Baier, S. Helama, and W. Oschmann (2007), ENSO-coupled precipitation records (1959–2004) based on shells of freshwater bivalve mollusks (*Margaritifera falcata*) from British Columbia, *Int. J. Earth Sci.*, *96*, 525–540.
- Smith, E., and G. Dent (Eds.) (2005), *Modern Raman Spectroscopy: A Practical Approach*, John Wiley, Hoboken, N. J.
- Stemmer, K., and G. Nehrke (2014), The distribution of polyenes in the shell of *Arctica islandica* from North Atlantic localities: A confocal Raman microscopy study, *J. Molluscan Stud.*, doi:10.1093/mollus/eyu033. [Available at <http://mollus.oxfordjournals.org/content/early/2014/06/09/mollus.eyu033.full.pdf>.]
- Wall, M., and G. Nehrke (2012), Identification of two organic bands showing different chemical composition within the skeleton of *Porites lutea*: A confocal Raman microscopy study, *Biogeosci. Discuss.*, *9*, 8273–8306.
- Wanamaker Jr, A. D., A. Baker, P. G. Butler, C. A. Richardson, J. D. Scourse, I. Ridgway, and D. J. Reynolds (2009), A novel method for imaging internal growth patterns in marine mollusks: A fluorescence case study on the aragonitic shell of the marine bivalve *Arctica islandica* (Linnaeus), *Limnol. Oceanogr.*, *7*, 673–681.
- Webb, G. E., G. J. Price, L. D. Nothdurft, L. Deer, and L. Rintoul (2007), Cryptic meteoric diagenesis in freshwater bivalves: Implications for radiocarbon dating, *Geology*, *35*, 803–806.
- Wehrmeister, U., D. E. Jacob, A. L. Soldati, N. Loges, T. Häger, and W. Hofmeister (2010), Amorphous, nanocrystalline and crystalline calcium carbonates in biological materials, *J. Raman Spectrosc.*, *42*, 926–935.